Small-angle x-ray scattering studies on nonionic microemulsions

Tsuyoshi Shimobouji, Hideki Matsuoka, and Norio Ise*
Department of Polymer Chemistry, Kyoto University, Kyoto 606, Japan

Hideo Oikawa
Research Laboratory, Dic-Hercules Chemicals, Inc., Yahatakaigan-dori, Ichihara, Chiba 290, Japan
(Received 31 March 1988)

The microstructure in a [*n*-dodecyltetraoxyethylene glycol monoether ($C_{12}E_4$)]-water-hexadecane system was investigated by the small-angle x-ray scattering (SAXS) technique for various surfactant concentrations and solution temperatures at a constant ratio of water and hexadecane (1:1 by weight). At 25 °C, a sharp distinct peak was observed in the SAXS curves. On the basis of the analysis of the surfactant concentration dependence of the peak position, it was concluded that a lamella structure had been formed. At 45 °C, the scattering curves showed a single, broad peak. With increasing $C_{12}E_4$ concentration, the peak position shifted toward higher angles. An analysis of the peak position suggested that oil-in-water (*O-W*) -type microemulsion droplets had been formed. At lower surfactant concentrations, the possibilities, that *W-O* droplets had been formed and that a bicontinuous structure had been constructed at the intermediate concentrations, were pointed out. The scattering profiles were not in contradiction with the theoretical ones for spheres if the polydispersity was considered. From a consideration of the peak position, which is related to the interparticle distance through the Bragg equation, it was suggested that the (spherical) droplets were distributed in a more or less ordered manner, probably in fcc or bcc symmetry, and not in simple-cubic symmetry. The radius and the aggregation number of the droplet were estimated to be about 13–17 Å and 35–1400, respectively, depending on the surfactant concentration.

I. INTRODUCTION

It is well known that in water-oil-surfactant systems (sometimes with a cosurfactant, usually alcohol), so-called microemulsions are formed.[1,2] The solutions are macroscopically but not microscopically, homogeneous; there must exist water regions, oil regions, and interface regions containing surfactant. Usually, the phase behavior is complicated, being a function of the surfactant concentration, salinity, solution temperature, etc. Some model structures have been proposed such as water droplets in oil (*W-O*), oil droplets in water (*O-W*), bicontinuous structures by Schwarz,[3] and by Scriven,[4] and a layer bicontinuous model by Shinoda.[5] For systems containing ionic surfactants, extensive work has been done.[6] However, for systems containing nonionic surfactant we can find only a few papers.[7] Furthermore, although small-angle x-ray and neutron-scattering techniques (SAXS and SANS) are the most powerful ones for the investigation of the microstructure of the systems under consideration, these techniques have not been used as often as they should be. In this paper, we perform a SAXS investigation on the microstructure of (*n*-dodecyltetraoxyethylene glycol monoether)-hexadecane-water systems as functions of the surfactant concentration and of the solution temperature.

II. EXPERIMENT

A. Materials

Dodecyltetraoxyethylene glycol monoether ($C_{12}E_4$, Scheme I) was purchased from Nikko Chemicals Inc., and used without further purification. (Scheme I)

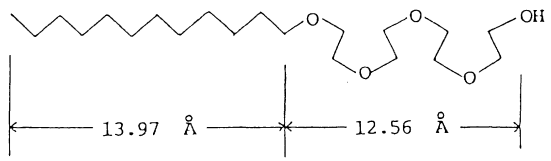

$C_{12}E_4$ (n-dodecyltetraoxyethylene glycol monoether).

Hexadecane was of a guaranteed grade of Wako Chemicals. The water used was a highly purified one obtained by a Millipore Milli-Q system. We prepared the three-component systems as follows: a suitable amount of $C_{12}E_4$ was dissolved in hexadecane, and water was added into the solution. The mixture was shaken by a Boltex mixer for a few seconds. Thereafter the solution was heated on a water bath up to about 40 °C, and then was controlled to the temperature required. The mixtures were usually kept standing in test tubes for about 24 h before the SAXS measurements. In the case of solutions which were highly viscous probably because of lamella structure (in the $L\alpha$ region to be discussed below), the solutions were warmed slightly before the SAXS measurements and transferred into observation SAXS cells (glass capillaries). The influence of the standing time was briefly checked by increasing the time to one month; no appreciable change in the peak position was noted.

B. SAXS apparatus

The SAXS apparatus and data processing system have been fully described elsewhere.[8] Cu $K\alpha$ radiation and a Ni filter were used.

III. RESULTS

A. Phase diagram

Figure 1 shows the phase diagram of the $C_{12}E_4$-hexadecane-water system obtained by eye observation. The ratio of water and hexadecane was fixed at 1:1 by weight. Three distinct phases, the 1Φ, 2Φ, and $L\alpha$ regions according to the terminology by Lichterfeld *et al.*,[7] were observed when the temperature and the surfactant content were varied. In the 2Φ region, the solution was separated into two phases; the water-rich phase and hexadecane-rich phase. In the 1Φ region, the solutions were one-phase clear ones and their viscosity was not so high. (The viscosity was estimated qualitatively by a test tube observation.) The $L\alpha$ region was also clear, being one phase but its viscosity was fairly high. The SAXS measurements were performed at the conditions indicated by circles in the phase diagram.

B. SAXS curves at 45 °C

Figure 2 shows SAXS curves of $C_{12}E_4$-water-hexadecane systems in the 1Φ region at 45 °C at various surfactant contents (line 1 in Fig. 1). The abscissa is the scattering vector S [$S=4\pi(\sin\theta)/\lambda$, where 2θ is the scattering angle and λ the wavelength of x ray] and the ordinate is the relative intensity of scattered x rays. For all scattering curves, a single, broad but distinct peak was observed. The peak position depended on the surfactant concentration; with increasing surfactant concentration, the peak position shifted towards higher angles.

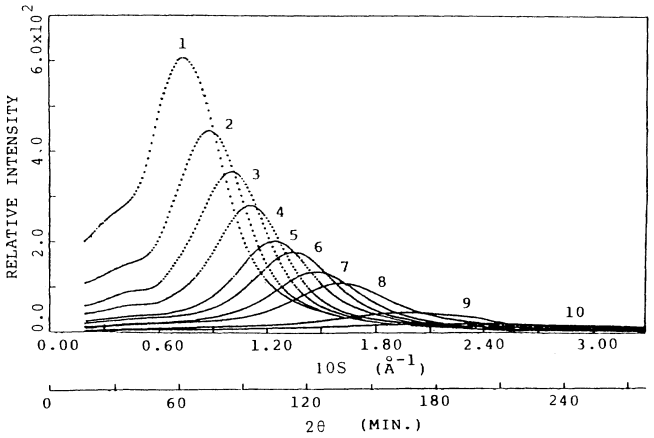

FIG. 2. Scattering curves of $C_{12}E_4$-water-hexadecane systems at 45 °C, water:hexadecane=1:1. Curve 1, [$C_{12}E_4$]=45 wt. %; 2, 50%; 3, 55%; 4, 60%; 5, 65%; 6, 70%; 7, 75%; 8, 80%; 9, 90%; 10, 100%.

C. SAXS curves at 37 °C

Figure 3 shows SAXS curves at 37 °C (line 2 in Fig. 1). The solution was in the 1Φ region except at [$C_{12}E_4$]=60 wt. %, which is in the $L\alpha$ region (see Fig. 1). A single broad peak, which is similar to those in Fig. 1, was observed. At [$C_{12}E_4$]=60 wt. %, the peak was discontinuously sharp. The wiggles near the base line at small-angle regions might be due to noise.

D. SAXS curves at 27 °C

Figure 4 shows the SAXS curves at 27 °C for various surfactant concentrations (line 3 in Fig. 1). Except at [$C_{12}E_4$]=80 wt. % (which is in the 1Φ region), the solu-

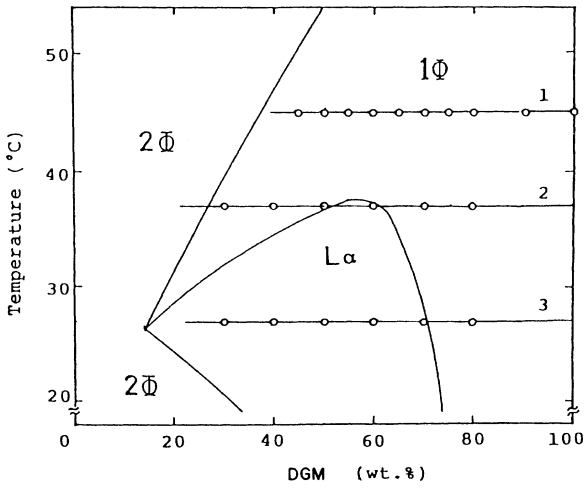

FIG. 1. Phase diagram of $C_{12}E_4$-water-hexadecane system, water:hexadecane=1:1.

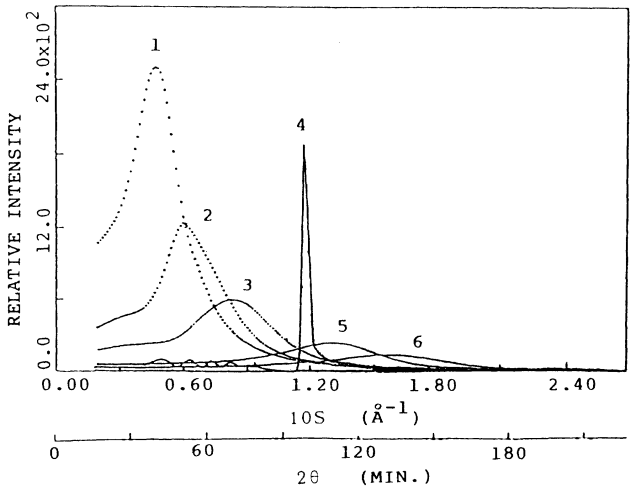

FIG. 3. Scattering curves of $C_{12}E_4$-water-hexadecane systems at 37 °C, water:hexadecane=1:1. Curve 1, [$C_{12}E_4$]=30 wt. %; 2, 40%; 3, 50%; 4, 50%; 4, 60%; 5, 70%; 6, 80%.

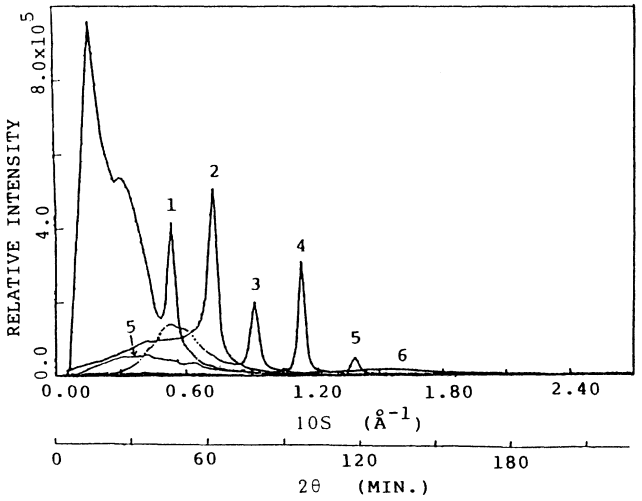

FIG. 4. Scattering curves of $C_{12}E_4$-water-hexadecane systems at 27 °C, water:hexadecane=1:1. Curve 1, $[C_{12}E_4]$=30 wt. %; 2, 40%; 3, 50%; 4, 60%; 5, 70%; 6, 80%.

tions were in the clear, one-phase $L\alpha$ region, but showed high viscosity. For all SAXS curves, a distinct sharp peak can be observed, which may mean that there exists some ordered structure in the solution. The position of the peak shifted towards higher angles with increasing $C_{12}E_4$ concentration. Except at $[C_{12}E_4]$=60 wt. %, another broad peak was observable at smaller-angle regions. For $[C_{12}E_4]$=60 wt. %, at which the $L\alpha$ phase can be maintained in a wide temperature range (up to 37°C) as is easily recognized from the phase diagram (Fig. 1), there was no broad peak at small-angle regions; only a sharp peak was observed.

IV. DISCUSSION

A. Microstructure in the $L\alpha$ region

A distinct sharp peak was observed for the SAXS curves in the $L\alpha$ region. These sharp peaks remind us of the existence of an ordered structure such as a lamella structure in the solutions. This is consistent with the high viscosity of the solution in the $L\alpha$ region. When a lamella structure is formed, the following relation holds:[3]

$$\Phi_s=(2v_s)/(a_H d) , \tag{1}$$

where Φ_s is the volume fraction of the surfactant, v_s is the volume of the surfactant molecule, a_H is the effective area of the cross section of the surfactant head group, and d is the length of the repeating unit. Equation (1) is derived for the lamella structure in which there are two surfactant molecules in the cylinder whose length is d and cross section a_H. The following relation between the scattering vector at the peak position (S_m) and d holds for a one-dimensional periodicity such as a lamella structure:

$$d=2\pi/S_m . \tag{2}$$

Substituting Eq. (2) into Eq. (1), we obtain

$$S_m=(a_H\pi/v_s)\Phi_s . \tag{3}$$

Equation (3) indicates that, if a lamella structure is maintained, the S_m versus Φ_s plot must be a straight line which goes through the origin with the slope $(a_H\pi/v_s)$.

In Fig. 5 the S_m of the sharp peaks at higher angles is plotted against Φ_s. A very good linearity passing through the origin can be observed, indicating that a lamella-like structure might exist in the $L\alpha$ region. Another broad peak observed at the small-angle region in Fig. 4 may suggest that another structure is maintained in solutions. Because the position and the height of the broad peak depend on the Φ_s, the content of the structure, which is the origin of the broad peak, might change. The excellent linearity in Fig. 5 involving all points may suggest that the densities in the lamella structure and in the coexisting structure are identical. However, no further information about the structure causing the broad peak at small-angle regions could be obtained by these experiments only. From the slope of the line in Fig. 5, as easily recognized from Eq. (3), we can evaluate the a_H value, which was calculated to be 38.5 Å^2. We used 601.3 Å^3 for the v_s value in this calculation at 25 °C, for example. Lichterfeld *et al.* reported that the a_H value of $C_{12}E_5$ was 42.9 Å^2 in the $L\alpha$ structure.[7] Thus, our a_H value, which was slightly smaller than the value for $C_{12}E_5$, was thought to be a reasonable one.

The peak height reflects the stability and the degree of order of the structure. However, the apparent peak height in Fig. 4 seems not to have any regularity except that the lamella structure is thought to be most stable at 60 wt. %. Although we cannot claim it in a conclusive way at this stage, this may be due to the coexistence of the other structure in addition to the lamella structure. In other words, the sharp scattering peak contains the contributions of the scattering from the lamella structure and from the other structure. Another possibility is that the system has a large, highly arranged lamella domain.[9]

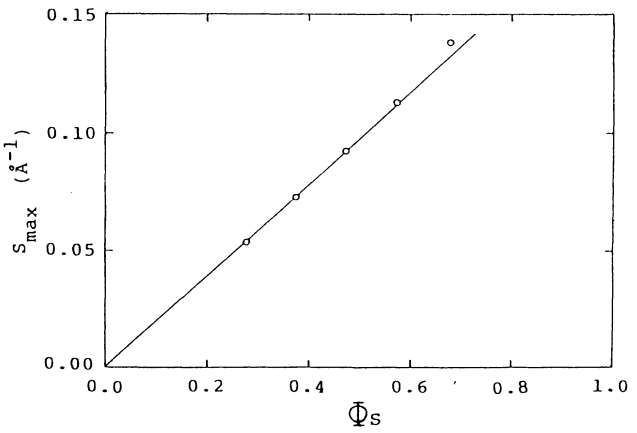

FIG. 5. S_{max} vs Φ_s plots for $C_{12}E_4$-water-hexadecane systems in the $L\alpha$ region, water:hexadecane=1:1.

In this case, a small difference in the angle between the orientation axis of the structure and the x-ray beam would affect the height of the lamella peak. Furthermore, needless to say, the scattering intensity ought to be normalized for the composition, which is not possible here due to the coexistence of the other structure.

Another puzzling feature is that we did not observe higher-order scattering peaks; we could observe only *one sharp* peak. This may suggest that the structure is highly ordered in the short range, but not in the long range. However, the real cause of the situation is still unclear.

B. Microstructure in the 1Φ region

A single, broad peak was observed for the SAXS curve of the solutions in the 1Φ region as shown in Fig. 2. The 1Φ region is a clear one-phase solution as in the $L\alpha$ region, but the viscosity of the solution is much lower than the latter. Therefore, it may be appropriate to consider whether water-in-oil (*W-O*)-type or oil-in-water (*O-W*) -type microemulsion droplets are formed in the solution. If there exist droplets in the 1Φ region, at least two possibilities must be considered for the origin of the peak; one is interparticle interference between the microemulsion droplets and the other is intraparticle interference of the droplets due to a heterogeneity of the density inside the particle. It is well known that there often appears a single broad peak in the scattering curve from a so-called core-shell-like particle [a particle which has a core surrounded by a shell of a scattering density different from the core such as the sodium dodecylsulfate (SDS) micelles for x-ray scattering[10]].

To clarify the origin of the peak, we examined the dependence of the SAXS curves on the number of droplets. Figure 6 shows the SAXS curves at various concentrations of $C_{12}E_4$ and water, while the ratio of these two components was kept constant; in other words, the figure shows the dependence of the SAXS curve on the droplet number, because the number of droplets [which were assumed to be of spherical water-in-oil (*W-O*) type] was determined by the volume of the water and the surface area covered by the head group of the surfactant, the area being determined by the value of a_H and the number of surfactant molecule. Thus, with increasing content of $C_{12}E_4$ and water, the number of *W-O* type droplets increased, while the size of the droplets did not change significantly. At small numbers of droplets (curve 1 and 2), the scattered intensity decreased monotonically with increasing scattering vector. However, at $[C_{12}E_4+\text{water}]=30$ wt. %, there appears a shoulder in the scattering curve, and at 40 wt. %, a single broad, but distinct, peak was observed. From this fact, the broad peak may be interpreted as due to interparticle interference effect, confirming that the particles (droplets) form a more or less regular distribution, as was discussed in a separate paper.[11] If the peak is due to an intraparticle interference effect, the peak would appear in all the scattering curves in Fig. 6 at the same position. This, however, was not experimentally the case.

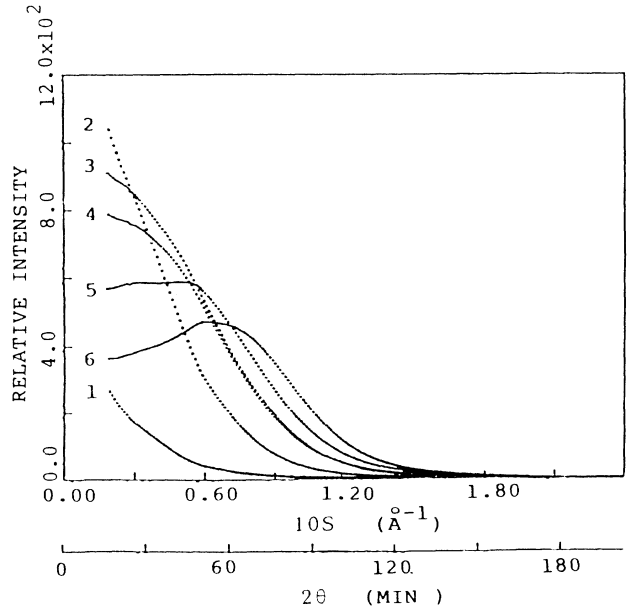

FIG. 6. Scattering curves of $C_{12}E_4$-water-hexadecane systems at 37 °C, water:$C_{12}E_4$ = 1:4. Curve 1, [water + $C_{12}E_4$] = 5 wt. %, 2, 10%; 3, 15%; 4, 20%; 5, 30%; 6, 40%.

When droplets are formed, the following relations must hold:

$$n=\Phi_c/(\tfrac{4}{3}\pi R^3)\,, \tag{4}$$

$$N=\Phi_s/(v_s n)\,, \tag{5}$$

$$a_H=(4\pi R^2)/N\,, \tag{6}$$

where Φ_c is the volume fraction of the droplets, n is the number of droplets per unit volume in the solution, R is the radius of the droplet, and N is the aggregation number.

When the droplets are arranged in a face-centered-cubic (fcc) or body-centered-cubic (bcc) lattice, the value of the scattering vector at the first peak position S_m and the nearest-neighbor interparticle distance D satisfy the following equation based on the scattering theory:

$$S_m=(\pi/\sqrt{6})/D\,. \tag{7}$$

From the packing requirement, we obtain

$$R=\alpha D\Phi_c^{1/3}\,, \tag{8}$$

where α is 0.5527 for fcc and 0.5685 for bcc lattices. Combining Eqs. (4)–(8), we obtain

$$S_m=(\pi\sqrt{6}\alpha a_H/3v_s)(\Phi_s/\Phi_c^{2/3})\,. \tag{9}$$

This equation shows that, if the peak is due to interparticle (interdroplet) interference, the S_m versus $\Phi_s/\Phi_c^{2/3}$ plot must be a striaght line which passes through the origin. From the slope of the line, we can evaluate the a_H value, if the v_s value is known.

Figure 7 shows the plot of S_m value as a function of $\Phi_s/\Phi_c^{2/3}$. Since the Φ_c value is different whether *W-O* droplets or *O-W* droplets are assumed, two plots are given in Fig. 7. When the *O-W* droplet formation is assumed, the plot shows an excellent linearity (filled circles

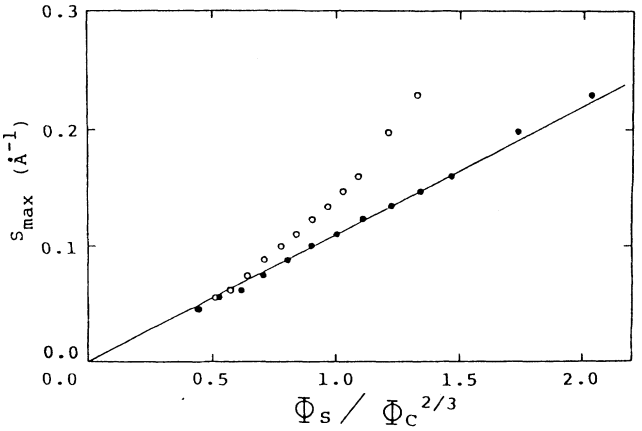

FIG. 7. S_{max} vs $\Phi_s/\Phi_c^{2/3}$ plots for $C_{12}E_4$-water-hexadecane systems in the 1Φ region, water:hexadecane=1:1. ○, *W-O* droplets; ●, *O-W* droplets.

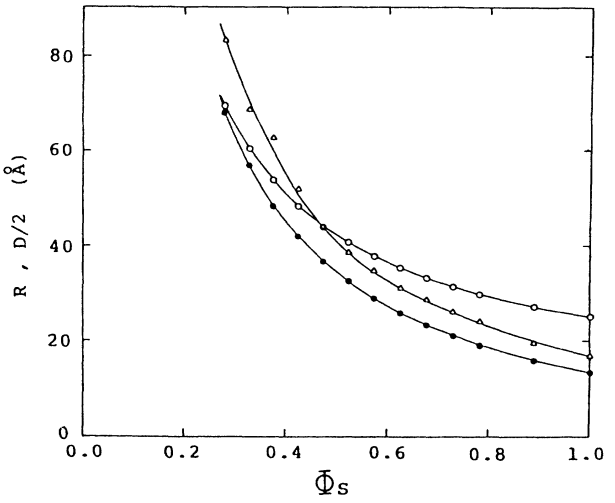

FIG. 9. R and $D/2$ values for $C_{12}E_4$-water-hexadecane microemulsion droplets at various surfactant concentrations, water:hexadecane=1:1, a_H=46.65 Å^2. △, $D/2$ from SAXS peak; ○, R values calculated from the mixing ratio for *W-O* droplets; ●, R values calculated from the mixing ratio for *O-W* droplets.

in Fig. 7). This suggests that the formation of *O-W* droplets is plausible under all conditions studied here. However, at small surfactant conditions, the formation of *W-O* droplets cannot be excluded, because the open circles in Fig. 7, calculated on the assumption of *W-O* droplets, fell also on the same straight line. Thus, we cannot distinguish here which of *O-W* or *W-O* droplets are formed at low surfactant conditions. From the slope of the line in Fig. 7, we can estimate the a_H value in the 1Φ region, which is calculated to be 46.7 Å for fcc and 45.4 Å for bcc lattice systems. These a_H values are larger than that (38.5 Å) in the $L\alpha$ region, which is reasonable because the curvature of the interfacial region is smaller than that of the lamella structure.

The relationship plotted in Fig. 7 does not enable us to distinguish the difference between *O-W* and *W-O* droplets. So we tried another method of analysis. We calculated Φ_c values using the measured S_m value, and demonstrate them in Fig. 8 as a function of the Φ_s values. The two straight lines show the calculated values from the composition of the solution. For large Φ_s values (>0.5), the plots show an excellent agreement with the line 2, which was calculated for the *O-W* droplets. However, at small Φ_s values, the plots deviated from the line 2, and fell on the line 1, which is for the *W-O* droplets. This may suggest the possibility that there occurs a transition from *O-W* droplets to *W-O* droplets with decreasing Φ_s.

If there occurs a transition from the *O-W* to the *W-O* droplets and vice versa, an intermediate structure such as a bicontinuous structure may be formed at the intermediate condition.[12,13]

Figure 9 shows the R value (the radius of the droplet)

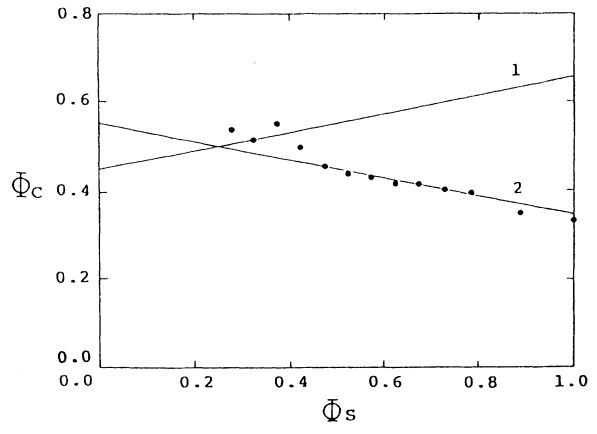

FIG. 8. Φ_c vs Φ_s plots for $C_{12}E_4$-water-hexadecane systems in the 1Φ region, water:hexadecane=1:1. Line 1, calculated from mixing ratio for *W-O* droplets; line 2, calculated from mixing ratio for *O-W* droplets.

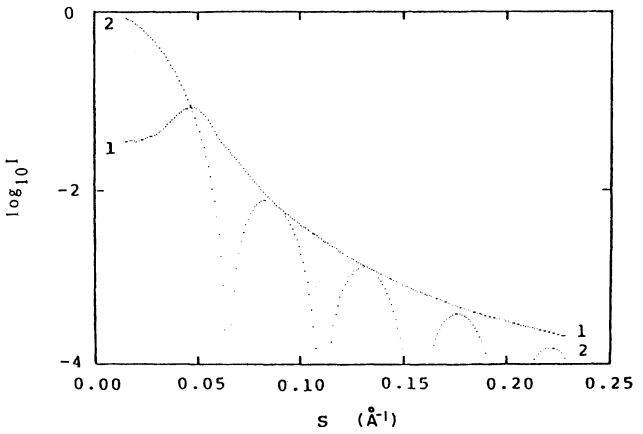

FIG. 10. Comparison of the experimental scattering curve of $C_{12}E_4$-water-hexadecane system and the theoretical scattering curve of a sphere. Curve 1, experimental scattering curve at 33 °C. Water:hexadecane=1:1, [$C_{12}E_4$]=30 wt. %; 2, Theoretical scattering curve of sphere of a radius of 70.4 Å.

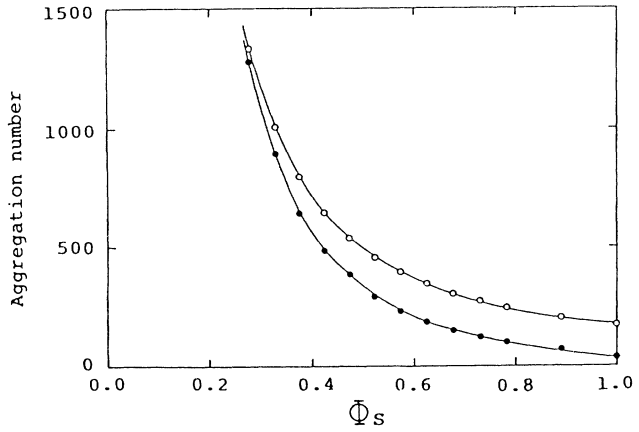

FIG. 11. Aggregation numbers of $C_{12}E_4$-water-hexadecane microemulsions at various surfactant concentrations calculated from the mixing ratio, water:hexadecane=1:1, a_H=46.65 Å^2. ○, *W-O* droplets; ●, *O-W* droplets.

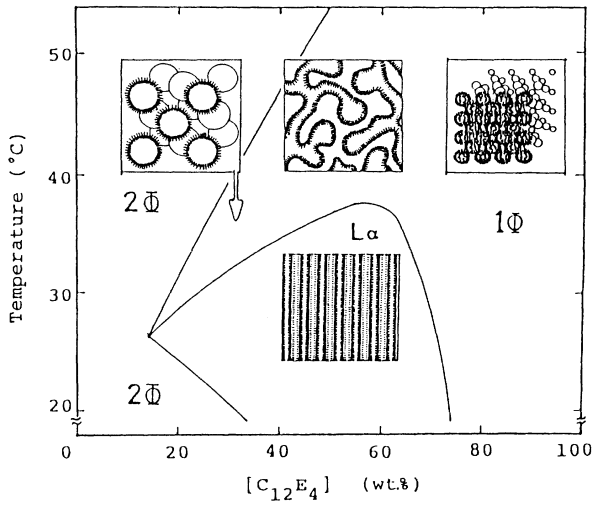

FIG. 12. Schematic diagram of the microstructure in $C_{12}E_4$-water-hexadecane system as function of the surfactant concentration and temperature. In the $L\alpha$ region at low temperatures, a lamella structure is formed, which shows a sharp peak in SAXS curve. In the 1Φ region, microemulsion droplets are formed and are arranged in a more or less ordered manner, hence the SAXS curve shows a single broad peak. *W-O* and *O-W* droplets are formed at low- and high-surfactant concentrations, respectively. At intermediate concentrations, a bicontinuous structure is formed as an intermediate state.

calculated by Eqs. (4)–(6). The $D/2$ values, the half of the interparticle distance, which were obtained from the number of the droplets with the assumption of a uniform distribution, are also shown. The R value decreases with increasing surfactant concentration for both *W-O* and *O-W* droplets. At low surfactant concentrations ($\Phi_s < 0.47$), the R values for both *W-O* and *O-W* droplets are smaller than the $D/2$ value, indicating that both types of droplets can exist. However, at high surfactant concentrations ($\Phi_s > 0.47$), the R value for the *W-O* droplet becomes larger than $D/2$. This situation is physically impossible. Thus, we can conclude that *W-O* droplets cannot be formed when the surfactant concentration is larger than 0.47. In Fig. 9, the $D/2$ value was evaluated for fcc and bcc systems. It is to be noted that, if a simple cubic (sc) system is assumed, the R values obtained were in most cases larger than the $D/2$ values for both the *O-W* and *W-O* droplets. Such a situation is physically not possible so that the sc systems may be ruled out.

In this calculation of the R values, we assumed that the droplets were perfectly spherical and monodisperse. However, such a situation cannot be real. Figure 10 shows a comparison of the experimental scattering curve for $[C_{12}E_4]$=30 wt.% and the theoretical scattering curve of a monodisperse sphere of radius 70.4 Å. The theoretical curve shows some higher-order maxima which are typical for a perfect isolated sphere. The origin of these peaks is an intraparticle interference effect at higher angles and is not due to the interparticle interference. When the shape of the particle deviates from a sphere and/or the particles are polydisperse, these maxima become smeared.[14] The tops of the maxima could be well reproduced by the experimental curve, suggesting that the droplets are spheres (although not perfect ones), whose mean radius is about 70.4 Å, and/or that they have some polydispersity. A quantitative estimation of the polydispersity would become possible by using the method of Hashimoto *et al.*[14] If we can find the particle-scattering function, it would be possible to obtain the so-called interparticle interference function, which describes the distribution of the droplets in solution more exactly. Such an analysis is now in progress.

Figure 11 shows the aggregation number (N) calculated from Eqs. (4) and (5) as a function of Φ_s. At low surfactant concentrations, the N value is fairly large—more than one thousand. With increasing Φ_s value, the N value becomes smaller down to 35.

V. CONCLUSION

In summary, we draw the schematic diagram of the microstructure of $C_{12}E_4$-water-hexadecane system shown in Fig. 12. The $L\alpha$ region, which appeared at low temperatures in the surfactant concentration range of 14–74 wt.%, had a lamella structure with a distance between repeating units of 45–117 Å. In the 1Φ region, which was observable at fairly high solution temperatures, the following structures were suggested; *W-O* droplets in low-surfactant-concentration conditions, *O-W* droplets in high surfactant conditions, and a bicontinuous structure at the intermediate condition, although the possibility of *O-W* droplet formation under all conditions could not be completely denied. The scattering profiles gave a good fit with the theoretical ones for spheres, whose radius is 70.4 Å at the surfactant concentration 30 wt.% (*W-O*-type droplet), for example, although it is implausible that the droplet is perfectly monodisperse. The droplets are distributed in a more or less distorted fcc or bcc lattice structure, which is the origin of the single broad SAXS peaks.

*Author to whom correspondence should be addressed.

[1]L. M. Prince, *Microemulsions, Theory and Practice* (Academic, New York, 1977).

[2]K. Shinoda and B. Lindman, Langmuir **3**, 135 (1987).

[3]H. A. Schwarz, *Gesammelte Mathematische Abhandlung* (Springer-Verlag, Berlin, 1890), Vol. 1, pp. 6–25.

[4]L. E. Scriven, in *Micellization, Solubilization, and Microemulsion,* edited by K. Mittal (Plenum, New York, 1977), p. 877.

[5]K. Shinoda, Progr. Colloid Polymer Sci. **68**, 1 (1983).

[6]For example, D. J. Cebula, R. H. Ottewill, J. Ralston, and P. N. Pusey, J. Chem. Soc. Faraday Trans. 1 **77**, 2585 (1981).

[7]F. Lichterfeld, T. Schmeling, and R. Strey, J. Phys. Chem. **90**, 5762 (1986).

[8]N. Ise, T. Okubo, S. Kunugi, H. Matsuoka, K. Yamamoto, and Y. Ishii, J. Chem. Phys. **81**, 3294 (1984).

[9]H. Urakawa (private communication).

[10]T. Zemb and P. Charpin, J. Phys. (Paris) **46**, 249 (1985).

[11]H. Matsuoka, H. Tanaka, T. Hashimoto, and N. Ise, Phys. Rev. B **36**, 1753 (1987).

[12]On the Φ_s dependence of S_m for a bicontinuous structure, the following relation has been proposed by Kotlarchyk *et al.* (Ref. 13): $S_m=(4a_H/3\sqrt{3}v_s)\Phi_s$. We applied this equation to our SAXS data in the 1Φ region, using the a_H value determined from Fig. 7. A fairly good agreement with the observed S_m was obtained for a few S_m values around $0.4<\Phi_s<0.5$. This might suggest that the bicontinuous structure is maintained in such a limited range of Φ_s if the same, constant a_H value is assumed.

[13]M. Kotlarchyk, S.-H. Chen, J. S. Huang, and M. W. Kim, Phys. Rev. Lett. **53**, 941 (1984).

[14]T. Hashimoto, M. Fujimura, and H. Kawai, Macromolecules **13**, 1660 (1980).